ChemBioChem

Research Article
doi.org/10.1002/cbic.202200413

Chemistry Europe
European Chemical Societies Publishing

www.chembiochem.org

Supramolecular Host-Guest Interaction-Driven Electrochemical Recognition for Pyrophosphate and Alkaline Phosphatase Analysis

Lingxia Qin,[a, c] Xinxin Ren,[a] Kaiyue Hu,[a] Di Wu,*[c] Zhiyong Guo,[a] Sui Wang,[a] Linwen Jiang,[a] and Yufang Hu*[a, b]

We report an electrochemical biosensor based on the supramolecular host-guest recognition between cucurbit[7]uril (CB[7]) and *L*-phenylalanine-Cu(II) complex for pyrophosphate (PPi) and alkaline phosphatase (ALP) analysis. First, *L*-Phe-Cu(II) complex is simply synthesized by the complexation of Cu(II) (metal node) with *L*-Phe (bioorganic ligand), which can be immobilized onto CB[7] modified electrode via host-guest interaction of CB[7] and *L*-Phe. In this process, the signal of the complex-triggered electro-catalytic reduction of H_2O_2 can be captured. Next, due to the strong chelation between PPi and Cu(II), a biosensing system of the model "PPi and Cu(II) premixing, then adding *L*-Phe" was designed and the platform was applied to PPi analysis by hampering the formation of *L*-Phe-Cu(II) complex. Along with ALP introduction, PPi can be hydrolyzed to orthophosphate (Pi), where abundant Cu(II) ions are released to form *L*-Phe-Cu(II) complex, which gives rise to the catalytic reaction of complex to H_2O_2 reduction. The quantitative analysis of H_2O_2, PPi and ALP activity was achieved successfully and the detection of limits are 0.067 μM, 0.42 μM and 0.09 mU/mL ($S/N = 3$), respectively. With its high sensitivity and selectivity, cost-effectiveness, and simplicity, our analytical system has great potential to for use in diagnosis and treatment of ALP-related diseases.

1. Introduction

Alkaline phosphatase (ALP), which is a kind of membrane-bound enzyme, can catalyze regularly the de- and trans-phosphorylation of phosphate-containing biomolecules,[1–3] which is involved usually for intracellular regulation and signal transduction in the process of cell apoptosis and growth.[4,5] Some recent studies show abnormal ALP expression has associated with various diseases (prostate cancer, liver disease, bone disease, *etc.*),[6,7] so ALP is one of the most broadly utilized biomarkers/indicators in ALP-related clinical diagnosis and disease treatment.[8,9] On the other hand, pyrophosphate ($P_2O_7^{4-}$, PPi) is a significant metabolite in many biochemical processes of human (Citrate/ATP hydrolysis, DNA replication, *etc.*), which can often act as a common substrate in ALP-dominated system.[10,11] Specially, PPi plays clinically an indispensable role in diagnosis and treatment of arthritic diseases,[12,13] and scientists can also make a definite diagnosis for chondrocalcinosis and dehydration crystal deposition of $Ca_2P_2O_7$ through the status of PPi in living cells.[14,15] Often, ALP and PPi tend to appear in biological system simultaneously and can be analyzed as a close associate team.[16,17] Up to now, varied methods have been designed for PPi and ALP detection, such as colorimetry,[18] fluorescence,[19] chemiluminescence,[20] and surface-enhanced Raman scattering.[21] Among these, some metal ions (including Zn(II), Cu(II), *etc.*) were used as medium/binding site, and the related strategy could be applied for ALP/PPi biosensing on the account of the strong chelation between metal ion and PPi.[22,23] However, this detection mechanism tends to occur in optical approaches, and to achieve on-site/point-of-care testing (similar to glucometer). Therefore, establishing a novel method for the detection of PPi and ALP activity through conducting electrochemical interface is needed and garners plenty of attention.

Supramolecular complexes have been developed rapidly owing to their excellent properties and wide applications in all fields.[24,25] Generally, these materials can be prepared through various noncovalent interactions, in which host-guest molecular recognitions are known as one of the most concerned non-covalent interactions. In this process, macrocyclic host (receptor) and guest (ligand) molecules with appropriate properties can be assembled to varied supramolecular systems.[26,27] What's really interesting is that the association and dissociation of supramolecular host-guest systems can be handled via numerous external stimulus.[28,29] Currently, plenty of macrocyclic host molecules (involving crown ethers, calix[n]arene, cyclophane, cucurbit[n]uril, cyclodextrin, pillar[n]arene, *etc.*) have been used

[a] *L. Qin, X. Ren, K. Hu, Z. Guo, S. Wang, L. Jiang, Y. Hu*
State Key Laboratory for Managing Biotic and Chemical Threats to the Quality and Safety of Agro-products
State Key Laboratory Base of Novel Functional Materials and Preparation Science, School of Materials Science & Chemical Engineering
Ningbo University, Ningbo, Zhejiang 315211 (P. R. China)
E-mail: huyufang@nbu.edu.cn
[b] *Y. Hu*
State Key Laboratory of Chemo/Biosensing and Chemometrics
College of Chemistry and Chemical Engineering
Hunan University, Changsha, Hunan 410082 (P. R. China)
[c] *L. Qin, D. Wu*
College of Medical Technology
Ningbo College of Health Sciences
Ningbo, Zhejiang 315100 (P. R. China)
E-mail: wudi8412@163.com

Supporting information for this article is available on the WWW under https://doi.org/10.1002/cbic.202200413

for the production of supramolecular complex with stimuli-responsive and selective abilities via amphiphilic, hydrogen bonding, electrostatic interactions, and so on.[30–32] Among these, cucurbit[n]urils (CB[n]s) have one hydrophobic cavity and two carbonyl-lined portals, which are a family of pumpkin-shaped macrocyclic host molecules.[33,34] Why is there a strong host-guest complexation force between CB[n] and certain molecule? There are two main factors: (1) the high-energy water captured in CB[n] cavity is released so as to lead to non-classical hydrophobic effect; (2) the electron-rich carbonyl portals of CB[n] is preferable binding with some guest molecules with positive charges due to the typical electrostatic attraction.[35,36] Among the family of CB[n]s, CB[7] can combine harmoniously with the majority of guest molecules owing to its low cytotoxicity and good aqueous dispersity.[37,38] For example, this cooperation between cavity and portal in CB[7] has been demonstrated to bind well with some special peptides (phenylalanine (Phe), tryptophan (Trp), tyrosine (Tyr), *etc.*).[39,40] Therefore, CB[7] is identified as a suitable host molecule to construct a new electrochemical biosensing interface based on host-guest interaction.

Herein, we describe firstly a new electrochemical biosensor for exploring PPi/ALP-dominated biological process on the basis of supramolecular host-guest interaction between CB[7] and a *L*-Phe-based complex and the detailed analysis processes are illustrated in Scheme 1. This method involves the following key parts: (1) Inspired by the combination of organic ligand and metal ion, *L*-phenylalanine-Cu(II) complex is synthesized by aromatic environment-caused hydrophobic interaction and both hydrogen bonding and Cu(II) chelation-resulted hydrophilic interaction; (2) *L*-Phe-Cu(II) complex not only has an excellent affinity with CB[7] modified interface in the view of supramolecular host-guest recognition but also displays good electro-catalytic activity to H_2O_2 reduction; (3) A new model of "PPi and Cu(II) premixing, then adding *L*-Phe" is employed for PPi analysis, in which the formation of typical PPi–Cu(II) complex can effectively hinder the synthesis of *L*-Phe-Cu(II) complex, thus leading to a "signal-off" mode; (4) Incorporation of ALP into PPi–Cu(II) complex can benefit from the regeneration of electrochemical signal because of a great deal of released Cu(II) ions via ALP-catalyzed hydrolysis to PPi, thus achieving indirectly the detection of ALP; meanwhile, the electrochemical signal can be affected again due to the introduction of ALP's inhibitor (Na_3VO_4), which can achieve the screening of inhibitor for ALP biosensing. The supramolecular host-guest recognition-dominated biosensor has excellent analytical performances and can be applied well in serum samples, indicating great prospect in a PPi/ALP-based biomedical analysis and clinical diagnosis.

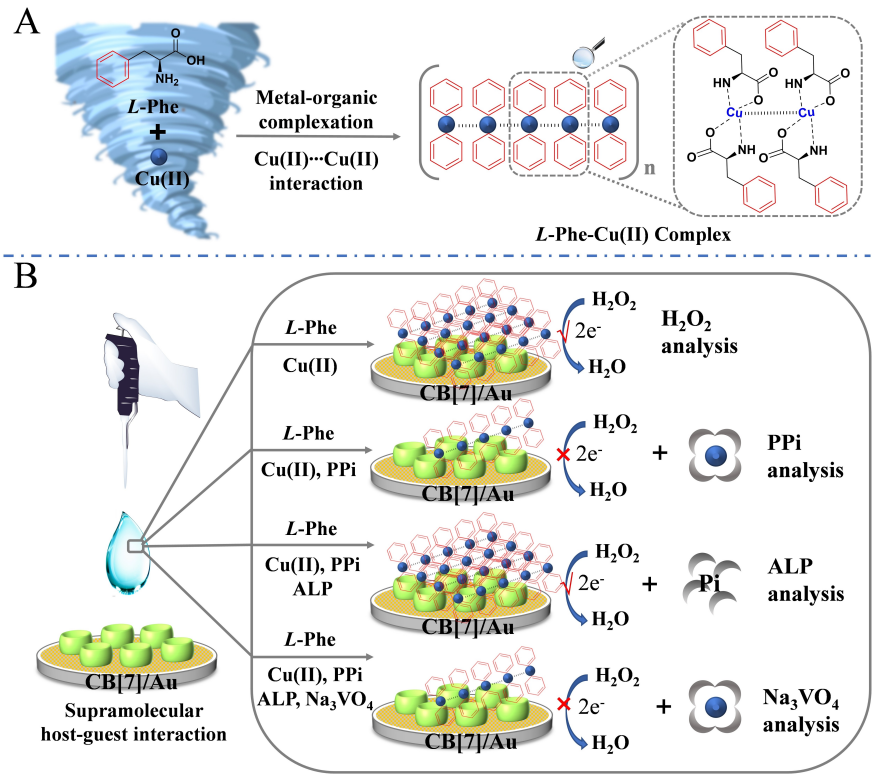

Scheme 1. Schematic illustrations of supramolecular host-guest interaction-driven electrochemical recognition: (A) the preparation of a unique complex of *L*-phenylalanine (*L*-Phe) and Cu(II); (B) pyrophosphate (PPi), alkaline phosphatase (ALP) and its inhibitor (Na_3VO_4) analysis based on the catalytic effect of the complex to H_2O_2.

Experimental Section

Reagents and apparatus

Alkaline phosphatase (ALP), trypsin, papain, cholesterol oxidase (ChOx), acetyl cholinesterase (AChE), urease, and cucurbit[7]uril (CB[7]) were obtained from the Aladdin Industrial Co. (Shanghai, China). Protein kinase A (PKA) and histone acetyltransferase (HAT) were obtained from Sigma-Aldrich Co. *L*-Phenylalanine (*L*-Phe) and $Na_4P_2O_7$ (PPi) were purchased from Sangon Biotech. Co. Ltd. (Shanghai, China). $CuSO_4 \cdot 5H_2O$ and H_2O_2 were from Sinopharm Chemical Reagent Co. Ltd. (China). Unless otherwise specified, all reagents used in our work were analytical reagent grade or higher. All solutions were prepared with double-distilled water (18.2 MΩ·cm) generated from the Millipore Milli-Q system.

All electrochemical experiments were carried out on a CHI 760E electrochemical workstation (Chenhua Instrument Company of Shanghai, China) by using a conventional three-electrode system (the working electrode, Au electrode (Au, 2 mm in diameter); the counter electrode, platinum wire electrode; the reference electrode, Ag/AgCl electrode). Size and zeta potential analysis was performed on Malvern Zetasizer Nano ZS90 (Malvern, UK). UV-vis spectra were measured with Shimadzu UV-1800 spectrophotometer (Kyoto, Japan). The morphologies of *L*-Phe-Cu(II) complex and its supramolecular structure were achieved by scanning electron microscopy (SEM, Hitachi SU-70 and Japan).

Synthesis of L-phenylalanine-Cu(II) complex

In a 1 mL of combination solution containing *L*-Phe (20 μM) and $CuSO_4 \cdot 5H_2O$ (200 μM), the synthesis of *L*-Phe-Cu(II) complex was carried out at 37 °C for 20 min under vigorous stirring (2800 rpm). After it, the mixture was centrifuged at 4 °C for 15 min under 13000 rpm to remove supernatant and redispersed to a total volume of 1 mL with double-distilled water.

Electrode fabrication

Prior to modification, the bare Au electrode was thoroughly polished on a chammy with 1.0 and 0.05 μm Al_2O_3 slurry, respectively, followed by sequentially sonication for 5 min each in water and ethanol, and then dried under N_2 condition. The electrode was noted as Au. Since CB[7] can spontaneously adsorb onto Au surfaces via physical adsorption and forms a stable monolayer,[41–43] the cleaned Au above was immersed in CB[7] (1 mM) aqueous solution for 12 h. Afterwards, it was washed gently for three times with the cleaning buffer (PBS, 10 mM, pH 7.0) and then dried under N_2 condition, which was labelled as CB[7]/Au. Finally, 5 μL of the synthesized *L*-Phe-Cu(II) complex above was added onto the surface of CB[7]/Au, and the electrode was put into 37 °C environment for 1 h and then rinsed with slowly the cleaning buffer to remove the residual complex. We named it complex/CB[7]/Au.

Electro-catalytic performance analysis of L-Phe-Cu(II) complex

Various final concentrations of H_2O_2 (0, 0.0001, 0.0002, 0.002, 0.005, 0.02, 0.05, 0.1, 0.5, 1, 2, 3, 4, 5, 5.5 and 6 mM) were added into PBS (0.1 M, pH 7.4). Subsequently, cyclic voltammograms (CVs) of complex/CB[7]/Au were performed in the prepared PBS (0.1 M, pH 7.4) containing H_2O_2, setting the potential range from −1.2 to 0 V with the scanning rate of 50 mV/s. Meanwhile, amperometric i-t curves were recorded in the 800 s by successive addition of H_2O_2 (0.6 μL, 1 mM) every 50 s at −0.8 V in a 2 mL of PBS (0.1 M, pH 7.4) under stirring.

PPi analysis

Initially, 10 μL of PPi with different final concentrations (0, 2, 10, 40, 80, 140, 200, 260, 320, 380, 440, 500 and 560 μM), 20 μL of Tris-HCl buffer solution (50 mM, pH 7.6), 10 μL of double-distilled water and Cu(II) (10 μL, 2 mM) were mixed at 37 °C for 1 h to combine sufficiently. Then, *L*-Phe (50 μL, 40 μM) was added to the reaction solution. In a volume of 100 μL, the final concentration of Cu(II) was maintained at 200 μM and the final concentration of *L*-Phe was kept at 20 μM. The rest of the experiment went as described in Section 2.2. Additionally, we replaced *L*-Phe-Cu(II) complex in Section 2.3 with the resulting solution here to discuss the role of PPi, but the other steps remained the same.

ALP activity and its inhibitor analysis

For ALP activity analysis, 10 μL of ALP with various final concentrations (0, 0.1, 0.5, 5, 10, 15, 20, 25, 30, 35, 40, 45 and 50 mU/mL), 20 μL of Tris-HCl buffer solution (50 mM, pH 7.6) and PPi (10 μL, 4.4 mM) was mixed and incubated at 37 °C for 1 h, and then of Cu(II) (10 μL, 2 mM) was added and the reaction was continued for another 1 h at 37 °C. Then *L*-Phe (50 μL, 40 μM) was added into the reaction solution above. The rest of the experiment was similar to describes above. The rest of the experiment was similar to Section 2.2. Additionally, we replaced *L*-Phe-Cu(II) complex as described in Section 2.3 with the resulting solution here to discuss the role of ALP, but the other steps remained the same.

In the study of ALP inhibition, 5 μL of Na_3VO_4 with different final concentrations (0, 5, 15, 30, 45, 60, 75, 90, 105, 120 and 150 μM) was premixed with 5 μL of ALP (final: 40 mU/mL) for 10 min. The subsequent ALP enzymatic reaction, the interaction of Cu(II) and PPi, and the combination of Cu(II) and *L*-Phe were consistent with the abovementioned ALP detection steps and conditions. Also, CV responses as a function of different concentrations of Na_3VO_4 were recorded.

Detection of PPi and ALP Content in goat serum samples

Unless otherwise specified, all real samples used in our work were goat serum. First, it should be noted that excess NaF solution should be added in real serum samples to eliminate the influence of pyrophosphatase (PPase) activity. Also, the detection of PPi or ALP content in real sample should be consistent with the step of PPi and ALP analysis above, but only the real serum samples were employed to take part in PPi or ALP analytical processes.

2. Results and Discussion

The feasibility verification on PPi and ALP analysis mainly focuses on the following parts: (1) successful synthesis of *L*-Phe-Cu(II) complex; (2) efficient assembly of complex/CB[7]/Au and its electro-catalytic capacity to the reduction of H_2O_2; (3) a new model of "PPi and Cu(II) premixing, then adding *L*-Phe" for PPi analysis; and (4) the hydrolysis of ALP to PPi and inhibition effect of ALP activity.

2.1. Characterization of L-Phe-Cu(II) complex and its host-guest interaction with CB[7]

A series of characterization experiments were performed to verify the formation of *L*-Phe-Cu(II) complex and its host-guest interaction with CB[7], involving DLS, UV-vis spectroscopy and SEM experiments. As shown in Figure 1A, the average hydrodynamic diameter significantly increases to *ca.* 218±39 nm after the metal-organic complexation of *L*-Phe and Cu(II). While the average hydrodynamic diameter further increases to *ca.* 1573±211 nm in the presence of CB[7], which is greater than that of sole *L*-Phe-Cu(II) complex. Meanwhile, it can be seen that along with the interaction of *L*-Phe and Cu(II), the zeta potential of the *L*-Phe-Cu(II) complex becomes more positive than sole *L*-Phe and sole Cu(II). But after supramolecular host-guest interaction between the complex and CB[7], the zeta potential gets smaller than that of sole *L*-Phe-Cu(II) complex due to the CB[7]'s cavity surrounded by carbonyl groups (Figure 1B). Next, we compare the UV-vis absorption spectra of *L*-Phe, *L*-Phe-Cu(II) complex and the combination of the complex and CB[7] (Figure 1C). Compared with sole *L*-Phe (black curve), a new absorption band at around 662 nm is exhibited at *L*-Phe-Cu(II) complex (red curve) or the combination of the complex and CB[7] (blue curve), which can be ascribed to the charge transfer between *L*-Phe and Cu(II).[44] Meanwhile, a high and wide shoulder peak at around 300 nm is observed under the complex of *L*-Phe-Cu(II) and CB[7] due to the bridge of certain interaction such as hydrogen bonding and electrostatic interactions.[44,45] In addition, the morphologies of *L*-Phe-Cu(II) complex before and after host-guest interaction with CB[7] were analyzed by SEM. Figure 1D illustrates that the assembled *L*-Phe-Cu(II) complex shows flexible ribbon structure, while *L*-Phe-Cu(II) complex after host-guest interaction with CB[7] displays a thick blocky shape due to the binding effect of CB[7]. According to the previous work,[44] we believe that the synthesized *L*-Phe-Cu(II) complex possesses a highly periodic structure, whose matrix units are constructed through hydrophobic (aromatic environment) and hydrophilic (hydrogen bond and Cu(II) coordination) interactions; on the other hand, supramolecular host-guest interaction recognition is achieved favorably by the unique cooperation on the cavity and portal of CB[7] with the *L*-Phe.

2.2. Fabrication of complex/CB[7]/Au and its catalytic reduction to H_2O_2

Recently, electrochemical sensors for H_2O_2 are constructed based on a synergistic catalytic mechanism of complex, including oxidation of metal centers and simultaneous reduction of hydrogen peroxide; in addition, copper metal ions are active agents of redox processes with several stable oxidation states, and Cu(II)-supported complex shows good potential for electrochemical applications.[46–48] In the view of the successful synthesis of *L*-Phe-Cu(II) complex and its host-guest interaction with CB[7], we expect *L*-Phe-Cu(II) complex can be attached stably onto CB[7]/Au surface, and subsequent verification is carried out by typical electrochemical method including electro-

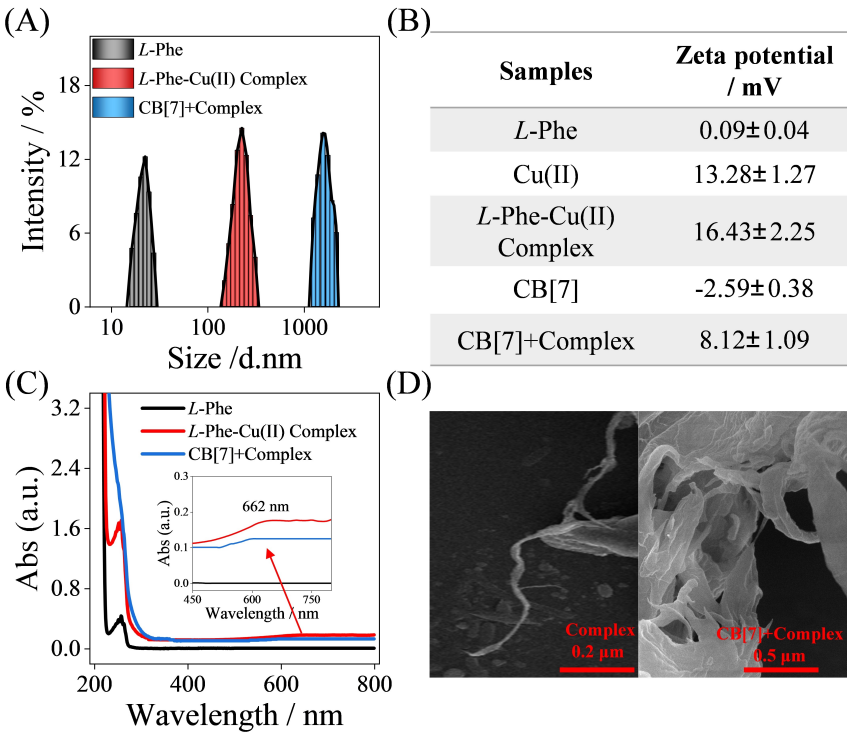

Samples	Zeta potential / mV
L-Phe	0.09±0.04
Cu(II)	13.28±1.27
L-Phe-Cu(II) Complex	16.43±2.25
CB[7]	-2.59±0.38
CB[7]+Complex	8.12±1.09

Figure 1. Characterization of *L*-Phe-Cu(II) complex and the combination of complex and CB[7]: (A) Size distributions and (B) Zeta potential determined by dynamic light scattering (DLS); (C) UV-vis absorption spectra; and (D) SEM images.

chemical impedance spectroscopy (EIS) and cyclic voltammetry (CV). As illustrated in Figure S1A, EIS response is monitored and labelled by electron transfer resistance (Ret). The bare Au (black) exhibits a small semicircle, while a higher semicircle appears on CB[7]/Au (blue) due to the electron-rich carbonyl portals of CB[n], indicating the successful binding of CB[7] to the Au. After *L*-Phe-Cu(II) complex are coated onto CB[7]/Au, a small increase of Ret is observed due to abundant *L*-Phe biological molecules, but there is not a huge increase of Ret which benefits from Cu(II) with positive charge. Additionally, it shows a well-defined pair of redox peaks at the Au, and the CV signal of $[Fe(CN)_6]^{3-/4-}$ decreases due to the negative charge of CB[7] (Figure S1B). When *L*-Phe-Cu(II) complex is efficiently adsorbed on the surface of CB[7]/Au, the current decreases somewhat, but not much, because of *L*-Phe as biomolecule and Cu(II) with positive charge at the same time. The results of the CV are consistent with that of the EIS, which further confirms the successful fabrication of the biosensor based on supramolecular host-guest interaction.

Later, we industriously look for a link between *L*-Phe-Cu(II) complex and electrochemical signal output. Figure 2A shows the CVs of complex/CB[7]/Au in PBS (0.1 M, pH 7.4) with or without 5 mM H_2O_2. In the absence of H_2O_2, no reduction peak can be observed at complex/CB[7]/Au, while an obvious reduction peak is observed with addition of 5 mM H_2O_2, presenting an excellent electro-catalytic reduction to H_2O_2. So, what are the conditions for the electro-catalytic reduction of H_2O_2? We go further into the in-depth discussion for these ingredients in the proposed electrode. As depicted in Figure 2B, as the assembly orderly of CB[7] and *L*-Phe-Cu(II) complex on Au surface, only a strong electrochemical signal appears on complex/CB[7]/Au, hence we believe that the electro-catalytic factor comes from the complex. Moreover, we further investigate the role of *L*-Phe, Cu(II), and *L*-Phe-Cu(II) complex, respectively (Figure 2C). Similarly, compared with the strong electro-catalytic signal of complex/CB[7]/Au to H_2O_2, a smaller signal appears at Cu(II)/CB[7]/Au, but a negligible signal is observed at *L*-Phe/CB[7]/Au, which can attribute to the non-special absorption of Cu(II) in CB[7]. The results suggest that only a good combination of *L*-Phe and Cu(II) can stimulate an excellent electrochemical signal, and the main reason is that the synergistic catalytic mechanism of metal-organic complex involves oxidation of metal centers and simultaneous reduction of H_2O_2. It led us to wonder what forces cause the favorable immobilization of the complex on electrode surface. Interestingly, there is no CV signal at the electrode without CB[7] (namely complex/Au), on the contrary, a significant CV signal occurs at complex/CB[7]/Au (Figure 2D), indicating an excellent supramolecular host-guest recognition interaction between the complex and CB[7] again. It follows that the proposed biosensor (complex/CB[7]/Au) has been fabricated well, and can be applied for electro-catalytic to H_2O_2 successfully.

In view of these, we employ the complex/CB[7]/Au to discuss the CV response for different concentrations of H_2O_2.

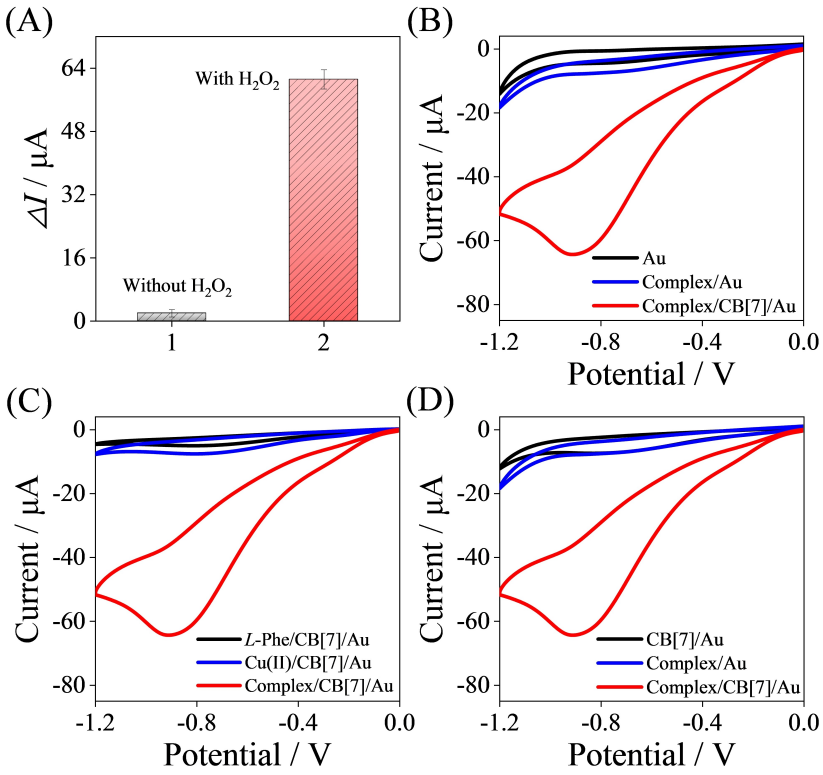

Figure 2. Cyclic voltammetry (CV) with a scanning rate of 50 mV/s in PBS containing 5 mM H_2O_2: (A) CV responses of complex/CB[7]/Au in the presence or absence of H_2O_2; (B) CV responses of the three-step assembly electrodes in the presence of H_2O_2; (C) CV responses of composition of the complex (such as *L*-Phe and Cu(II)) in the presence of H_2O_2; (D) CV responses of the modified electrodes with or without CB[7] in the presence of H_2O_2 to discuss the role of CB[7].

Before testing, we optimize the experimental conditions directing at the electrode fabrication. The ratio of *L*-Phe and Cu(II) has a great effect on the electro-catalytic reduction of H_2O_2, and as shown in Figure S2A, the maximum CV signal occurs in the ratio of 1: 10, then a plateau comes, which is chosen for the synthesis of *L*-Phe-Cu(II) complex. In a similar way, 1 mM of CB[7] concentration, and 1 h of incubation time and 37 °C of incubation temperature between the complex and CB[7]/Au are received favorably (Figure S2B, S2 C, and S2D). Subsequently, it can be seen from Figure 3A that the reduction peak current of H_2O_2 increases as the concentration increasing from 0 to 6 mM. The fitting curves of the CV current to H_2O_2 concentration are obtained in the range of 0.0002 to 5 mM with a detection limit (LOD) of 0.067 μM ($S/N = 3$) (Figure 3B). These results indicate that *L*-Phe-Cu(II) complex has a good electro-catalytic activity, making it a viable electrochemical sensing material for H_2O_2 detection. Compared with other H_2O_2-targeted methods in Table S1, the sensitivity of our electrochemical assay is more excellent. We hypothesize that the outstanding electro-catalytic property of complex/CB[7]/Au can be attributed to two factors: the *L*-Phe-Cu(II) complex attached by CB[7] can provide not only plenty of adsorption sites for ·OH species of H_2O_2 but also a good-sized, naked catalytic surface which can act as highly active electro-catalysts.[49–51]

Furthermore, to ensure high efficient electro-catalytic reaction and continuous stable output signal, H_2O_2 (0.6 μL,1 mM) is continuously added to PBS (0.1 M, pH 7.4) every 50 s to test amperometric i-t responses of complex/CB[7]/Au (Figure 3C). Under a fixed potential of −0.8 V, it can be seen that the complex/CB[7]/Au exhibits a fast response with the change in H_2O_2 concentration, but other electrodes display a slight change of current, which is a sharp contrast. This further proves well the successful assembly of electrode, the stable electro-catalytic capacity of the complex and the binding between complex and CB[7]. In addition, the specificity for H_2O_2 is elucidated by comparing it with several other substances (ascorbic acid (AA), citric acid (CA), uric acid (UA), dopamine (DA), glucose (GLU), sucrose (SUC)). A significant change in current occurs after the addition of H_2O_2 (0.6 μL,1 mM), while the currents are almost unchanged after the same addition of other interferents (Figure 3D), illustrating that these interferents cannot be captured by complex/CB[7]/Au and cannot affect the reduction of H_2O_2. Subsequently, by taking five of the same biosensors under four concentration levels of H_2O_2, the biosensor exhibits good reproducibility (Figure S3A). Repeatability is also the basic evaluation indicator of electrochemical biosensor, so five electrodes are tested under the same conditions by comparing their CV responses to H_2O_2. As shown in Figure S3B, the differences in the displayed CV responses are negligible, implying an excellent repeatability. We also investigate the stability of biosensors, and CV measurements are taken after storage for every 3 days at 4 °C (Figure S3C). After a month, the CV current still keeps 87.4% of the original current with a relative standard deviation (RSD) of 4.27%, indicating that the

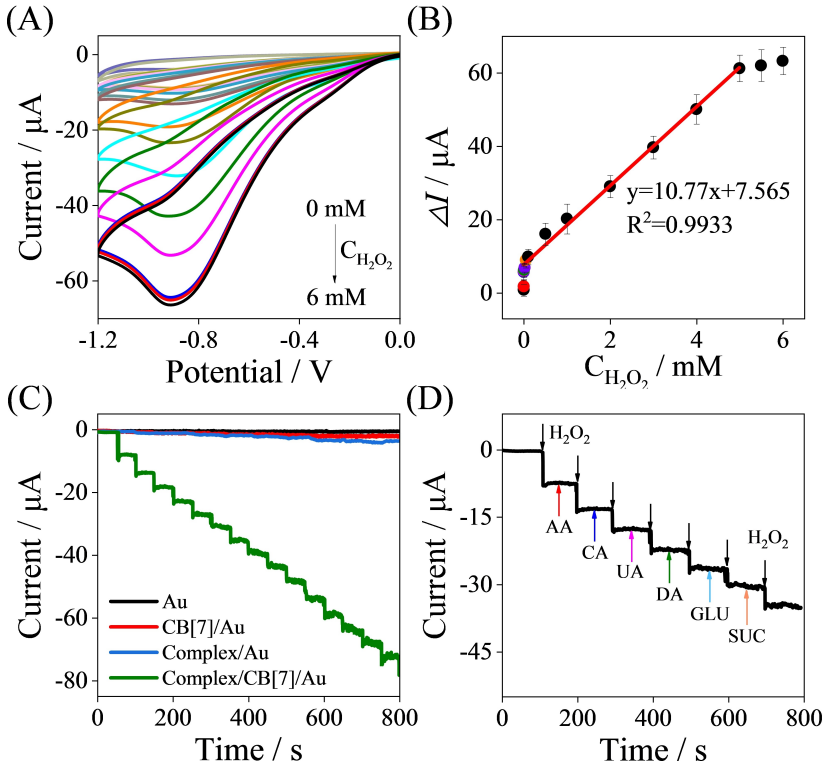

Figure 3. Detection of H_2O_2: (A) CVs of the complex/CB[7]/Au in the presence of H_2O_2 with different concentrations (final: 0, 0.0001, 0.0002, 0.002, 0.005, 0.02, 0.05, 0.1, 0.5, 1, 2, 3, 4, 5, 5.5 and 6 mM); (B) the linear relationship between the CV current and the concentration of H_2O_2. (C) Amperometric i-t responses of different modified electrodes on the successive addition of H_2O_2 (0.6 μL, 1 mM) in 0.1 M PBS (pH 7.4) solution. (D) Amperometric i-t responses at complex/CB[7]/Au on the alternating successive addition of H_2O_2 (0.6 μL, 1 mM) and other substances with the same content (AA, CA, UA, DA, GLU and SUC).

complex/CB[7]/Au is considerable stable. Nevertheless, the developed biosensor should not only be accomplished in the lab but also needs to meet the real sample analysis, so we design recovery experiments for different concentrations of H_2O_2 in serum samples, and the results are shown in Table S2. Satisfactory recoveries (from 97.2% to 103.4%) and well-pleasing RSDs (from 1.4% to 3.2%) are obtained, indicating that the biosensor has potential applications for H_2O_2 analysis in practical application.

2.3. Detection of PPi, ALP and its inhibitors

Generally, Cu(II) has a strong binding with PPi and there is a higher stability constant (K) of Cu(II)-PPi complex ($\log K_{Cu\text{-}PPi} = 12.45$),[52] but Cu(II) and *L*-Phe also can occur metal-organic complexation to some extent. So, the competitive cohesion of PPi and *L*-Phe to Cu(II) decides the direction of our strategy. As shown in Figure 4A, we set four combinations based on the interaction of Cu(II), *L*-Phe and PPi, and the model of "two of them premixing, then adding the third substance" is designed. For combination 3, a great decline of CV current is observed relative to combination 4 (without PPi), presenting a higher interaction of Cu(II) and PPi. But in three factors system, whether PPi is mixed with Cu(II) first (combination 1), or PPi is mixed with *L*-Phe first (combination 2), the corresponding current is very closer to the background, suggesting a preferentially binding of PPi to Cu(II) relative to *L*-Phe. Therefore, the model of "PPi and Cu(II) premixing, then adding the *L*-Phe" is employed in the following experiments. Then, we found that only in the absence of PPi, the CV signal will be more obvious, otherwise the CV signal is extremely weak (Figure 4B). These results indicate that our strategy can further be applied for PPi analysis. Before it, we optimize the interaction time, the interaction temperature and the reaction ratio of PPi and Cu(II) (Figure S4), the optimal incubation time, temperature and ratio is 1.0 h, 37 °C and 2.2: 1, respectively. Under the optimal conditions, the changes of CV current at complex/CB[7]/Au are recorded after the addition of PPi with different concentrations from 0 to 560 μM (Figure 4C), and the CV responses gradually decrease along with an increasing concentration of PPi. A good linear relationship is received between the CV response and PPi concentration in the range from 2 to 440 μM (Figure 4D), and the LOD is calculated to 0.42 μM ($S/N = 3$), which was superior to most values reported in the literature (Table S3).

To further evaluate the specificity of PPi biosensor, some potential interferences are studied by the replacement of target. Only there is a decline of the CV response in the presence of PPi, but other controls have almost no influence over CV signal (Figure S5A). It can be ascribed to the strong and effective chelation effect between PPi and Cu(II). Meanwhile, the anti-interference of the strategy is designed by the way to coexist with PPi. Compared with the case of sole PPi, no CV signal changes are observed with other interferents (Figure S5B), and

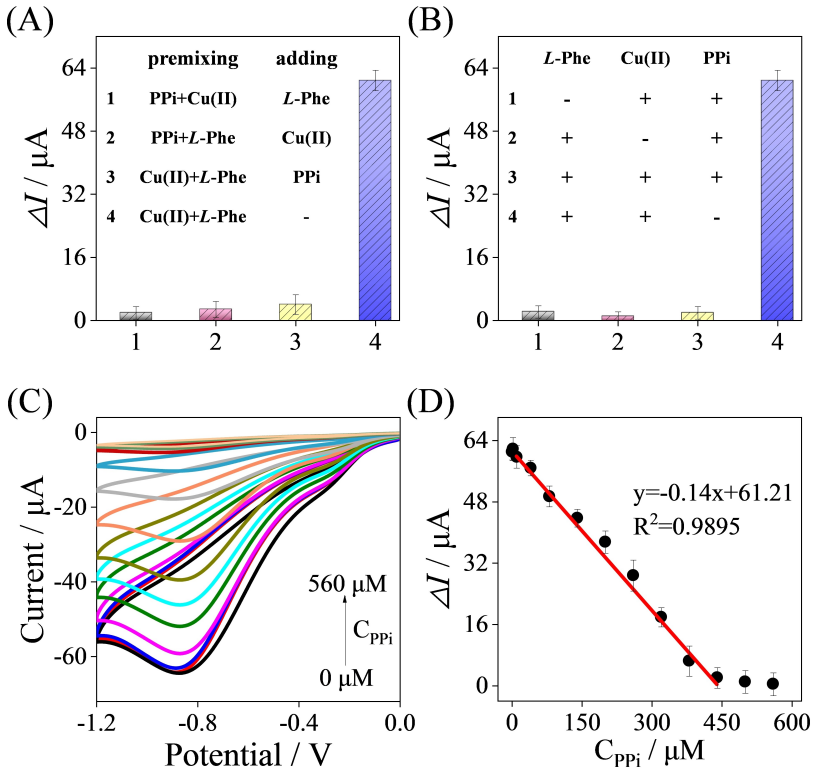

Figure 4. Detection of PPi: (A) CV responses to discuss the relationship of *L*-Phe, Cu(II), and PPi, any two of the three are pre-mixed and one is added later, inset: mixed sequential presentation; (B) CV responses to investigate the missing ingredient in this PPi analytical system, inset: ingredient list presentation; (C) CVs of the complex/CB[7]/Au with different concentrations of PPi (final: 0, 2, 10, 40, 80, 140, 200, 260, 320, 380, 440, 500 and 560 μM) with in PBS (0.1 M, pH 7.4) containing 5 mM H_2O_2; (D) the linear relationship between the CV current and the concentration of PPi.

the reason is the inability of these interferents to bind with Cu(II) tightly. Furthermore, five proposed biosensors with four concentration levels of PPi are used to assess the reproducibility, and as shown in Figure S5C, the biosensor displays good reproducibility. Next, as illustrated in Figure S5D, five electrodes show negligible differences in CV response for PPi detection, indicating a good repeatability of our proposed biosensor. After one month, PPi testing results have no obvious changes with a RSD of 1.46% (Figure S5E), which can attribute to a "signal-off" mode of PPi detection, and demonstrate that the biosensor can be applied in detecting PPi with acceptable stability. Next, the practicability of complex/CB[7]/Au is evaluated by monitoring PPi in serum sample. As summarized in Table S4, recoveries of 98.4%~103.6% are achieved with RSDs of no more than 4%.

ALP is closely relevant to certain critical diseases, and ALP and PPi are often discussed together, illustrating great feasibility for ALP analysis. In our system, ALP can catalyze hydrolysis of PPi to result in no PPi–Cu(II) complex. Firstly, to achieve the optimum effect for probing ALP, several experimental parameters, including incubation time and temperature of ALP, and pH of ALP reaction buffer are systematically optimized (Figure S6). Finally, incubation time of 60 min and temperature of 37 °C for ALP catalytic reaction, and pH of 7.6 for enzymatic reaction buffer are selected because of the best CV signal. After it, we test the CV current in the presence or absence of ALP (Figure 5A), and an obvious CV current appears under ALP condition, verifying the feasibility of our method to ALP detection. Furthermore, we also discuss several major compo-

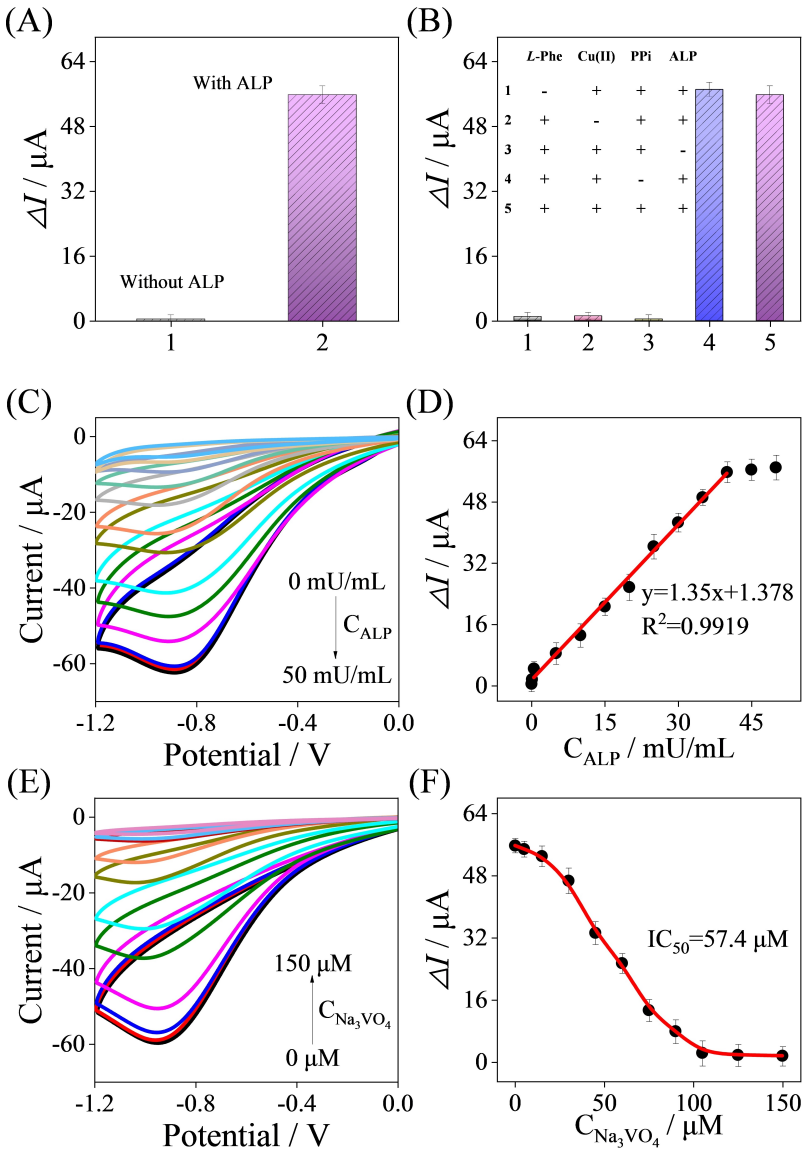

Figure 5. Detection of ALP: (A) CV responses of complex/CB[7]/Au in the presence or absence of ALP; (B) CV responses to investigate the missing ingredient in this ALP analytical system, inset: ingredient list presentation; (C) CVs of the complex/CB[7]/Au under ALP with different concentrations (final: 0, 0.1, 0.5, 5, 10, 15, 20, 25, 30, 35, 40, 45 and 50 mU/mL) in PBS (0.1 M, pH 7.4) containing 5 mM H_2O_2; (D) the linear relationship between the CV current and the concentrations of ALP; (E) CVs of the complex/CB[7]/Au under Na_3VO_4 with different concentrations (final: 0, 5, 15, 30, 45, 60, 75, 90, 105, 120 and 150 μM) in PBS (0.1 M, pH 7.4) containing 5 mM H_2O_2; (F) CV responses as a function of the concentration of Na_3VO_4.

nents designed into the system (Figure 5B). When *L*-Phe and Cu(II) cannot bind well under PPi condition (combination 1, 2, and 3), the CV signal is the same to that of PPi biosensor. But *L*-Phe-Cu(II) complex can form favorably in the presence of ALP due to lack of substate for hydrolysis (combination 4), and the role of PPi in ALP catalysis is pointed out favorably. It is worth noting that for the combination 5, the CV responses do not almost decrease in the presence of PPi, which can be ascribed to the hydrolysis of PPi catalyzed by ALP. As expected, with the increase of the ALP concentration up to 50 mU/mL, the CV response on ALP is found to rise gradually (Figure 5C). There is a linear relationship between the CV response and the ALP concentration from 0.5 to 40 mU/mL (Figure 5D). The LOD is evaluated to be 0.09 mU/mL ($S/N = 3$), which is lower than other methods for ALP detection (Table S5). Afterwards, to test whether the ALP assay can quantitatively explore the inhibitors of ALP, Na_3VO_4 (a potent small molecule inhibitor of ALP) is chosen for model. Briefly, by premixing a series of different concentrations of Na_3VO_4 in the ALP system, we found that the ALP activity is significantly inhibited with the addition of Na_3VO_4, and the corresponding CV signal decreases correspondingly with Na_3VO_4 concentrations from 0 to 150 μM (Figure 5E). The relationship between CV responses and Na_3VO_4 concentrations is shown in Figure 5F. The IC_{50} value (half maximum inhibitory concentration of the inhibitor) is then determined to be 57.4 μM, which is similar with previous literatures (Table S5).

Selectivity and anti-interference of the method are key to the biosensing analysis. As shown in Figure S7A, the specificity of the biosensor for ALP is also verified by challenging with several proteins, including AChE, ChOx, urease, HAT, papain, PKA, and trypsin. The CV signal for ALP is much higher than that of other substances, indicating an excellent selectivity. The resistance to interference is then evaluated and illustrated in Figure S7B, and negligible CV signal changes could be observed relative to that of ALP alone, displaying an excellent anti-interference capacity. In addition, five biosensors with four concentration levels of ALP are used to assess the reproducibility of the method, and the tiny change of CV signals indicates good reproducibility (Figure S7C). As shown in Figure S7D, the differences in CV response for the five electrodes under the same conditions is negligible, indicating a good repeatability. After one month, the current response still maintains 89% of original current, and the RSD of the current response is 3.35% (Figure S7E), indicating that the electrochemical biosensor is an effective platform for sensitive detection of ALP. In addition, the developed biosensor is also applied to probing the ALP activity in serum samples. Different amounts of ALP are added in the diluted serum solution. As shown in Table S6, the recoveries of ALP in diluted serum samples vary from 97.9% to 102.5% for ALP activities in the range from 1 to 30 mU/mL. These results demonstrate the promising applications of the method in complex biological and clinical system.

3. Conclusions

In summary, a sensitive, selective and low-cost electrochemical biosensor is developed for the detection of PPi, ALP and its inhibitor on the basis of the supramolecular host-guest interaction between CB[7] and *L*-Phe-Cu(II) complex. Notably, the *L*-Phe-Cu(II) complex which possesses electro-catalytic capacity to H_2O_2 can be prepared by a simple and green method. Then, the complex can be attached onto electrochemical substrate owing to the host-guest recognition of CB[7] and *L*-Phe. Then, we use PPi–Cu(II) complex as a starting point, and a new biosensing method for PPi testing is constructed by hindering the formation of *L*-Phe-Cu(II) complex. Furthermore, the method is also applied for ALP analysis in the view of the hydrolysis to PPi. The proposed biosensors with high sensitivity and selectivity can be adapted not only to basic laboratory experiments, but also to actual sample analysis, which can be conducive to the diagnosis and treatment ALP-related diseases clinically.

Acknowledgements

Financial support from the National Natural Science Foundation of China (42076193), the Open Funds of Key Laboratory of Diagnosis and Treatment of Digestive System Tumors of Zhejiang Province (KFJJ-202201), the Ningbo Municipal Natural Science Foundation (202002N3178), Zhejiang Provincial Natural Science Foundation of China (LY20B050005), Scientific Research Project of Education Department of Zhejiang Province (Y202147697), and University-level Project of Ningbo College of Health Sciences (2019Y01) are gratefully acknowledged.

Conflict of Interest

The authors declare no conflict of interest.

Data Availability Statement

Research data are not shared.

Keywords: analytical methods · cucurbit[7]urils · electrochemical biosensing · *L*-Phe-Cu(II) complex · supramolecular host-guest interactions

[1] W. E. G. Müller, H. C. Schröder, X. Wang, *Chem. Rev.* **2019**, *119*, 12337–12374.
[2] M. Bekhit, T. Blazek, W. Gorski, *Anal. Chem.* **2021**, *93*, 14280–14286.
[3] S. Vimalraj, *Gene* **2020**, *754*, 144855.
[4] L. Dewangan, J. Korram, I. Karbhal, R. Nagwanshi, K. K. Ghosh, S. Pervez, M. L. Satnami, *Ind. Eng. Chem. Res.* **2022**, *61*, 3636–3646.
[5] L. Ding, T. Zhang, C. Dong, J. Ren, *Anal. Chem.* **2022**, *94*, 5181–5189.
[6] Y. Hu, Y. Miao, J. Zhang, Y. Chen, L. Qiu, J. Lin, D. Ye, *Nano Lett.* **2021**, *21*, 10377–10385.
[7] F. A. Bushira, S. A. Kitte, Y. Wang, H. Li, P. Wang, Y. Jin, *Anal. Chem.* **2021**, *93*, 15183–15191.

[8] X. Huang, X. Bian, L. Chen, L. Guo, B. Qiu, Z. Lin, *Anal. Chem.* **2021**, *93*, 10351–10357.
[9] L. Zhang, Y. Li, G. Mu, L. Yang, C. Ren, Z. Wang, Q. Guo, J. Liu, C. Yang, *Anal. Chem.* **2022**, *94*, 2236–2243.
[10] H. Zhang, Q. Ju, S. Pang, N. Wei, Y. Zhang, *Dyes Pigm.* **2021**, 194, 109569.
[11] Y. Zhan, S. Yang, L. Chen, Y. Zeng, L. Li, Z. Lin, L. Guo, W. Xu, *ACS Sustainable Chem. Eng.* **2021**, *9*, 12922–12929.
[12] H. Li, S. Zhang, M. Chen, J. Wang, *Sensor. Actuat. B Chem.* **2022**, *359*, 131574.
[13] Y. Chang, H. Qin, X. Wang, X. Li, M. Li, H. Yang, K. Xu, G. Qing, *ACS Sens.* **2020**, *5*, 2438–2447.
[14] L. Hou, Y. Huang, T. Lin, F. Ye, S. Zhao, *Biosens. Bioelectron.* **2022**, *10*, 100101.
[15] H. S. Al-mashriqi, H. Zheng, S. Qi, H. Zhai, *J. Mol. Struct.* **2021**, *1242*, 130755.
[16] L. Zhang, J. Zhao, M. Duan, H. Zhang, J. Jiang, R. Yu, *Anal. Chem.* **2013**, *85*, 3797–3801.
[17] C. Chen, D. Zhao, Y. Jiang, P. Ni, C. Zhang, B. Wang, F. Yang, Y. Lu, J. Sun, *Anal. Chem.* **2019**, *91*, 15017–15024.
[18] Q. Zhang, Y. Yu, X. Yun, B. Luo, H. Jiang, C. Chen, S. Wang, D. Min, *ACS Appl. Nano Mater.* **2020**, *3*, 5212–5219.
[19] H. Lu, S. Xu, *ACS Omega* **2021**, *6*, 16565–16572.
[20] N. Fan, P. Li, C. Wu, X. Wang, Y. Zhou, B. Tang, *ACS Appl. Bio Mater.* **2021**, *4*, 1740–1748.
[21] X. Dai, L. Lu, X. Zhang, Z. L. Song, W. Song, Q. Chao, Q. Li, W. Wang, J. Chen, G. C. Fan, X. Luo, *Sensor. Actuat. B* **2021**, *334*, 129605.
[22] F. Niu, Y. L. Ying, X. Hua, Y. Niu, Y. Xu, Y. T. Long, *Carbon* **2018**, *127*, 340–348.
[23] P. Das, N. B. Chandar, S. Chourey, H. Agarwalla, B. Ganguly, A. Das, *Inorg. Chem.* **2013**, *52*, 11034–11041.
[24] B. Hua, L. Shao, M. Li, H. Liang, F. Huang, *Acc. Chem. Res.* **2022**, *55*, 1025–1034.
[25] A. L. de Marco, D. Bochicchio, A. Gardin, G. Doni, G. M. Pavan, *ACS Nano* **2021**, *15*, 14229–14241.
[26] Z. Zhang, H. Liang, M. Li, L. Shao, B. Hua, *Org. Lett.* **2020**, *22*, 1552–1556.
[27] G. Yu, K. Jie, F. Huang, *Chem. Rev.* **2015**, *115*, 7240–7303.
[28] T. T. Kim Cuc, P. Q. Nhien, T. M. Khang, H. Y. Chen, C. H. Wu, B. T. B. Hue, Y. K. Li, J. I. Wu, H. C. Lin, *ACS Appl. Mater. Interfaces* **2021**, *13*, 20662–20680.
[29] Y. Mei, Q. W. Zhang, Q. Gu, Z. Liu, X. He, Y. Tian, *J. Am. Chem. Soc.* **2022**, *144*, 2351–2359.
[30] H. Wu, H. Wang, F. Qi, T. Xia, Y. Xia, J. F. Xu, X. Zhang, *ACS Appl. Mater. Interfaces* **2021**, *13*, 33962–33968.
[31] Q. Song, K. Zhao, T. Xue, S. Zhao, D. Pei, J. Nie, Y. Chang, *Macromolecules* **2021**, *54*, 8314–8320.
[32] H. Nie, Z. Wei, X. L. Ni, Y. Liu, *Chem. Rev.* **2022**, *122*, 9032–9077.
[33] C. B. Rodell, J. E. Mealy, J. A. Burdick, *Bioconjugate Chem.* **2015**, *26*, 2279–2289.
[34] F. N. Tehrani, K. I. Assaf, R. Hein, C. M. E. Jensen, T. C. Nugent, W. M. Nau, *ACS Catal.* **2022**, *12*, 2261–2269.
[35] R. X. Cheng, F. Y. Tian, L. X. Chen, Q. J. Zhu, K. Chen, Z. Tao, *Cryst. Growth Des.* **2022**, *22*, 747–750.
[36] S. J. Barrow, S. Kasera, M. J. Rowland, J. Del Barrio, O. A. Scherman, *Chem. Rev.* **2015**, *115*, 12320–12406.
[37] K. S. Chen, L. Qi, J. Chen, R. Wang, H. Z. Yu, *J. Phys. Chem. C* **2022**, *126*, 1661–1671.
[38] R. Andrýs, A. Klusoňová, M. Lísa, J. Kassa, J. Ž. Karasová, *Mol. Pharmacol.* **2021**, *18*, 2416–2427.
[39] G. Cheng, J. Luo, Y. Liu, X. Chen, Z. Wu, T. Chen, *ACS Appl. Bio Mater.* **2020**, *3*, 8211–8240.
[40] J. W. Lee, M. H. Shin, W. Mobley, A. R. Urbach, H. I. Kim, *J. Am. Chem. Soc.* **2015**, *137*, 15322–15329.
[41] D. W. Lee, K. M. Park, B. Gong, D. Shetty, J. K. Khedkar, K. Baek, J. Kim, S. H. Ryu, K. Kim, *Chem. Commun.* **2015**, *51*, 3098–3101.
[42] J. Zhao, S. Hu, W. Zhong, J. Wu, Z. Shen, Z. Chen, G. Li, *ACS Appl. Mater. Interfaces* **2014**, *6*, 7070–7075.
[43] P. Neirynck, J. Brinkmann, Q. An, D. W. J. van der Schaft, L. G. Milroy, P. Jonkheijm, L. Brunsveld, *Chem. Commun.* **2013**, *49*, 3679–3681.
[44] M. Liu, J. H. Yin, C. Lan, L. Meng, N. Xu, *Microchim. Acta* **2022**, *189*, 98.
[45] E. Delgado-Pinar, I. Pont, E. García-España, J. S. Seixas de Melo, *Phys. Chem. Chem. Phys.* **2022**, *24*, 2403–2411.
[46] A. Aleksovska, P. Lonnecke, E. Hey-Hawkins, *Dalton Trans.* **2020**, *49*, 4817–4823.
[47] Q. Zhang, Y. Hu, D. Wu, S. Ma, J. Wang, J. Rao, L. Xu, H. Xu, H. Shao, Z. Guo, S. Wang, *Talanta* **2018**, *183*, 258–267.
[48] S. J. Wang, F. Bigdeli, X. W. Yan, L. Esrafili, K. G. Liu, H. Ghasempour, X. Q. Cai, M. L. Hu, A. Morsali, *J. Organomet. Chem.* **2020**, *926*, 121507.
[49] S. Sarma, B. Devi, P. K. Bhattacharyya, D. K. Das, *J. Fluoresc.* **2020**, *30*, 1513–1521.
[50] S. Hu, Q. Shuai, Y. Lin, Y. Fu, M. Li, *Nanotechnology* **2022**, *33*, 135503.
[51] P. Makam, S. S. R. K. C. Yamijala, K. Tao, L. J. W. Shimon, D. S. Eisenberg, M. R. Sawaya, B. M. Wong, E. Gazit, *Nat. Catal.* **2019**, *2*, 977–985.
[52] J. B. English, A. E. Martell, R. J. Motekaitis, I. Murase, *Inorg. Chim. Acta* **1997**, *258*, 183–192.

Manuscript received: July 20, 2022
Revised manuscript received: August 20, 2022
Accepted manuscript online: August 23, 2022
Version of record online: September 8, 2022